Research Square

Preprints are preliminary reports that have not undergone peer review.
They should not be considered conclusive, used to inform clinical practice,
or referenced by the media as validated information.

Leucas Aspera leaves extract as a copper corrosion inhibitor in 0.5M H_2 SO_4 medium

Dr.S.Jyothi sankar
kumaraguru Institute of Engineerig and Technology
Dr.N.Kavitha narayanaperumal (kavithan@sriet.ac.in)
Sri Ranganathar Institute of Engineering and Technology

Research Article

Keywords: Leucas Aspera, EIS, SEM-EDXS, FT-IR

Posted Date: June 6th, 2023

DOI: https://doi.org/10.21203/rs.3.rs-2980472/v1

License: This work is licensed under a Creative Commons Attribution 4.0 International License.
Read Full License

Abstract

The corrosion inhibitive action of leaves extracts of *Leucas Aspera* on copper corrosion in 0.5M H_2SO_4 solution was studied using the weight-loss method, Potentiodynamic polarization, EIS measurements, SEM-EDXS and FT-IR spectroscopic techniques. The results obtained indicate that the extracts functioned as good inhibitors in 0.5M H_2SO_4 solution. The inhibition efficiency was found to increase with extract concentration. Potentiodynamic polarization curves indicated that the plant extracts behave as mixed-type inhibitors. The thermodynamic parameters showed that the adsorption of the extracts on copper is physical, spontaneous, and favoured at low temperatures. The data for the adsorption of extract fit well with Langmuir adsorption isotherm. FTIR results showed that the inhibition mechanism was by the absorption process, through the functional groups present in the extract. The SEM images of the corrosion product confirmed the protection offered by the extract on the surface of the metal immersed in the 0.5M H_2SO_4 medium.

1 Introduction

` Copper and its alloys have widespread industrial applications in both aqueous and non-aqueous media, due to their excellent physical, chemical, mechanical, and electrical properties [1]. They have high resistance against corrosion. Although it is a corrosion-resistant metal due to its relatively noble potential and a naturally forming oxide film, it is subject to corrosion in oxygen-containing environments and high concentrations of chloride, sulphate, nitrate, and sulphides [2]. The use of an inhibitor plays an important role in the corrosion protection of metal in acidic media. The inhibitor may be classified as cathodic, anodic, or mixed, depending on whether their influence is mainly in retarding the cathodic or anodic reaction of the corrosion process or both of them. As a result, they cause a shift of the corrosion potential of the inhibited metal toward respectively either the cathodic or the anodic directions or they substantially leave the metal corrosion potential more or less unchanged. The technical, economical, and environmental issues have prompted the researchers to go for green corrosion inhibitors. Natural products are a good source of green corrosion inhibitors, where most of their extracts containing the necessary elements such as O, N, C and S, which are active in organic compounds, assist in adsorption of these compounds on metals or alloys to form a film that protects the surface and hinders corrosion.

In recent days many researchers have been investigated by the corrosion behaviour of metals in different environments using various parts of the plants as corrosion inhibitors. The use of plant extracts as inhibitors for the corrosion of metals/alloys has gained very wide interest among researchers in recent times [3–19].

In this study, the extract of *Leucas Aspera* was utilized as an inhibitor of corrosion on copper in the methanolic H_2SO_4 medium. *Leucas Aspera* contains phytochemical constituents like alkaloids, phytosterols, flavonoids, saponins, phenols, and glycosides, which are responsible for its antibacterial, antioxidant, and cytotoxic effects [20]. Earlier, we reported the successful corrosion prevention of mild steel in HCl medium by methanol extract of *Leucas Aspera* leaves [21]. Thus, herein, we report the

inhibitive properties of methanol extract of *Leucas Aspera* leaves on the corrosion of copper in a 0.5 M H_2SO_4 medium.

2 Experimental Detail

2.1 Specimen preparation

The Cu specimen with a dimension of 1×5×0.24 cm and with an area of 12.98 cm^2 was used for the weight loss study and a specimen with an exposed area of 0.9785 cm^2 was used for the electrochemical study. The surface of the specimen was mechanically polished with different grades (600, 1000, 1500, and 2000) of emery papers washed successively with doubled distilled water, degreased with acetone, and stored in a desiccator for their application. The chemical composition of copper is used as follows: (wt. %) Cu- 93.41%,

Pb – 0.014%, Fe- 0.037%, Sn – 0.057%, Zn- 6.473%.

2.2 Extract preparation

Fresh LA leaves were picked and then cleaned with tap water to remove ash and mud, dried in the shade, and then ground into a powder. About 20g of the dried and powdered LA leaves were taken in a soxhlet and extracted with 140 ml of methanol in 500 ml RB flask for about 6 hr. Thereafter, the solution was evaporated to about 50 ml on a water bath. The concentrated extract was dried to complete dryness. The dark brown solid residue (about 0.25g) obtained was preserved in a desiccator. A stock solution of the methanol extract of *Leucas Aspera* (MLA) was prepared by dissolving the required weight of the residue in methanol. Desired concentrations of the (0.05–0.40 g/L) were obtained by properly diluting the stock solution with distilled water. The test solution was freshly prepared before each experiment.

2.3 Weight loss method

The pre-cleaned and pre-weighed Cu specimens in triplicate were suspended in a 100 ml test solution with and without inhibitor at different concentrations of MLA in 0.5M H_2SO_4 for a period of 1 h. After that, the specimens were taken out, washed with distilled water, dried, and weighed. From the weight loss data, percentage inhibition efficiency (% IE) was calculated. The experiments were performed for various parameters such as concentration of the inhibitor (0.05, 0.10, 0.15, 0.20, 0.25 g/L), temperature variation (303- 333K), corrosive media (H_2SO_4) and different immersion time (1, 5, 48, 72 hours). The percentage of inhibition efficiency (%IE), corrosion rate (CR), and surface coverage (θ) were obtained using the following equations.

$CR\ (mpy) = (K\Delta W) / \rho At$ (1),

$IE = (W_{(b)}\text{-}W_{(i)} / W_{(b)}) \times 100$ (2),

$(\theta) = (W_{(b)}\text{-}W_{(i)} / W_{(b)})$ (3),

where $W_{(b)}$ and $W_{(i)}$ are the values of weight loss without and with inhibitor respectively, ΔW is the weight loss in grams, ρ is the density of coupon in g cm^{-3}, A is the area of the coupon in cm^2 and t is the exposure period in hours.

2.4 Electrochemical method

Electrochemical measurements were performed using the electrochemical analyzer of CHI instruments (model 608D). The experiments were carried out in a three-electrode cell assembly consisting of a copper specimen that was used as the working electrode. Saturated calomel and a platinum wire mesh were used as a reference and auxiliary electrodes respectively. AC impendence studies were conducted in the frequency range of 10,000–1 Hz at the resting potential using 0.02V sine wave as the excitation signal. R_{ct} and C_{dl} values were obtained from the Nyquist plots. The % IE was calculated from the following equation.

$$(\%IE) = (R_{ct\,(i)} - R_{ct\,(b)})/R_{ct\,(i)}) \times 100 \quad (4),$$

where $R_{ct(b)}$is the charge transfer resistance in the absence of inhibitor and $R_{ct(i)}$ is the charge transfer resistance in the presence of inhibitor.

2.5 Polarization method

Potentiodynamic polarization studies were carried out in the potential range from − 0.3 to 0.2 V at a scan rate of 0.01 V $Sec.^{-1}$. The electrochemical parameters such as corrosion current density (I_{corr}), corrosion potential (E_{corr}), and anodic and Cathodic slopes (b_a and b_c) were obtained from Tafel plots, and the % IE was determined using the formula

$$(\%IE) = (I_{corr\,(b)} - I_{corr\,(i)}) / I_{corr\,(b)}) \times 100 \quad (5),$$

where $I_{corr(b)}$ is the corrosion current density in the absence of inhibitor and $I_{corr(i)}$ is the corrosion density in the presence of inhibitor.

2.6 SEM Surface Morphology

To investigate the influence of the inhibitor on the corrosion phenomenon of copper, the photographs of fresh, inhibited, and uninhibited copper samples were recorded using SEM-EDXS (ZEISS Sigma microscope 5th version). The pre-cleaned specimens were immersed for 72 h in the blank solution of 0.5 M H_2SO_4 without and with 0.25g/L MLA extract at 25°C and then washed with distilled water, dried in warm air and submitted for SEM surface examination.

3 Results and discussion

3.1 Weight loss method

The corrosion rate (CR) and inhibition efficiency (%IE) from weight loss studies of copper in 0.5M H_2SO_4 in the presence and absence of MLA at room temperature for various immersion times (1-72 h) at different concentrations are illustrated in Table1. It is evident from these results that inhibition efficiency increases and the corrosion rate decreases on the addition of plant extract with concentrations at all immersion times up to 72 h. This is due to the adsorbed layer of the inhibitor acts as a barrier between the copper metal surface and the acid solution, leading to a decreasing corrosion rate. It is found that %IE is 77.39 in 0.5 M H_2SO_4 for the highest inhibitor concentration of 0.25g/L even at a longer immersion time of 72 h. The increase of %IE with increasing the inhibitor concentration indicates more inhibitor molecules are adsorbed on the copper surface in both acid media by blocking more corrosion active sites. The enhanced % IE may be explained due to the increase of adsorbed of inhibitor molecules on the metal surface with time [22]. Fig.1 shows the variation of inhibition efficiency of MLA with its concentration in 0.5M H_2SO_4 medium.

3.1.1 Temperature studies and thermodynamic parameters

To evaluate the nature of adsorption of MLA and activation parameters of the corrosion process of copper in 0.5M H_2SO_4 medium, weight loss measurements were carried out at various temperatures (303, 313, 323 and 333 K) in the absence and presence of MLA at different concentrations for 1 h immersion time and the data are shown in Table 2. It is observed that when the temperature is increased, the %IE decreased from 68.96 to 26.53, which is due to physisorption. The variation of %IE with temperature for various concentrations of the inhibitor in 0.5 M H_2SO_4 is shown in Fig. 2. As the temperature is increased, the inhibition efficiency decreased at all concentrations. This shows that MLA prevents the dissolution of metal ions in aggressive acids through physical adsorption. The activation energy (E_a) for Cu corrosion reaction at different inhibitor concentrations was found out from the slope of the Arrhenius plot

(log CR vs. 1/T) (Fig. 3),

where the slope is E_a/2.303 R, CR is the corrosion rate, R is the gas constant, and T is the temperature in absolute scale. These values are summarized in Table 3.

E_a values are higher for an inhibited solution than for the uninhibited one. The increasing value of activation energy with increasing concentration of extract shows that there is adsorption of leaves extracts on to the copper surface that blocks the active sites of copper specimens resulting in a decreased corrosion rate. Further, the corrosion rate decreases with an increase in temperature due to desorption. This is an indication of spontaneous adsorption of the inhibitor molecules on the copper surface and is attributed to physisorption [23-24]. The increase in the activation energy of the inhibited system is due to the adsorption of the inhibitor molecules on active sites.

3.1.1.1 Adsorption Isotherm

The nature of the interaction between the inhibitor and metal surface can be clearly explained by the adsorption isotherm. Attempts were made to fit the experimental data to assorted isotherms including

Langmuir, Freundlich, Tempkin, Frumkin, El-awady, and Flory-Huggins. It has been found that the data fit well with the Langmuir adsorption isotherm (Fig. 4) with the correlation coefficient nearing almost unity.

The free energy of adsorption ΔG_{ads} for various concentrations of inhibitor at different temperatures was calculated using the following equation:

ΔG_{ads}= -RT ln K(6),

where K = θ /C_{inch} (1 - θ), θ is surface coverage, C_{inh} is the concentration of inhibitor. It is described in the literature that a value of ΔG_{ads}upto -20 kJ mol^{-1}or less negative implies that the adsorption is due to electrostatic interaction between charged molecules and a charged metal and the process indicates physical adsorption, while those more negative than -40KJmol^{-1} involves charge sharing or transfer from the inhibitor molecules to the metal surface to form a co-ordinate type of bond that indicates chemical adsorption [25]. Analysis of the data presented in Table 3 shows that the values of ΔG_{ads} are less negative than -20 kJ mol^{-1}suggesting physisorption. The negative value of ΔH_{ads} indicates that the adsorption of inhibitor molecules on the metal surface is an exothermic process. It is observed that ΔS_{ads} values in the presence of inhibitor are positive. This implies that the formation of the activated complex is the rate-determining step representing association rather than dissociation, indicating that a decrease in disorder on going on from reactants to the activated complex [26].

3.2 Electrochemical measurements

The corrosion behavior of copper in 0.5 M H_2SO_4 solution in the absence and presence of different concentrations of MLA was investigated using electrochemical measurements. The impedance data obtained from Nyquist plots for the above-mentioned systems are given in Table 4 and Fig. 5 (a). The impedance diagrams obtained for all the studied systems are not perfect semicircles. The imperfect semicircle (depressed semicircle) is attributed to the frequency dispersion as a result of the roughness and inhomogeneity of the electrode surface. This is an indication of the fact that the adsorption of the inhibitor molecules on the copper surface leads to the formation of a surface protective film, which reduces the corrosion active sites on the metal surface thus enhancing its corrosion resistance [27].

To get a more accurate fit for the experimental data, various circuits have been tried and the best accuracy is found with the simple Randles equivalent circuit. The Randles equivalent circuits used for impedance studies are given in Fig. 5 (b), where R_S is a solution resistance, C_{dl} is the double layer capacitance and $R_{ct}$is the charge transfer resistance. The electrochemical parameters of R_{ct}, $C_{dl,}$ and %IE in the presence and absence of MLA in 0.5 M H_2SO_4 are listed in Table 4. It is apparent from Table 4 that both the C_{dl} values and R_{ct}values increase with increasing the inhibitor concentration. The increase in R_{ct}in the presence of MLA is because the added inhibitor molecules displace the water molecules at the interface of the double layer leading to the transfer of charge from solution to the metal surface. The increase in C_{dl} values in the presence of the different concentrations of MLA compared to that of the

blank solution is due to the decrease in local dielectric constant and/or an increase in the thickness of the electrical double layer. This suggests the adsorption of inhibitor molecules at the metal/solution interface. The adsorption can occur directly based on donor-acceptor interactions between the lone pair of electrons, π electrons in MLA, and the vacant d orbital of copper atoms [28].

The current potential relationship for copper corrosion in 0.5 M H_2SO_4 with different concentrations of MLA was investigated through the polarization measurements and the important parameters (Table 4) were obtained from the Tafel plots (Fig. 5 (b)). The Tafel slopes were calculated by the linear extrapolation of the cathodic and anodic branch of the polarization curves. Corrosion current (I_{corr}) was calculated from the slope of the polarization curve (b_a and b_c)and linear polarization resistance R_p was calculated using the Stern-Geary equation

$$I_{corr} = [b_a\, b_c / 2.303(b_a + b_c)] \times (1/R_p) \quad (7)$$

The polarization data show the addition of the inhibitor alters both $b_a$and b_c values suggesting that the inhibitor reduces both anodic dissolutions of the metal and retard hydrogen evolution reaction. This indicates the mixed nature of the inhibitor. The I_{corr} values decrease while increasing the concentration of inhibitors, which represents the higher surface coverage of the inhibitors [29-30].

3.3 Surface analysis

3.3.1 SEM analysis

The SEM images of the pure Cu sample, samples exposed for 72 h in 0.5 M H_2SO_4, and those exposed for 72 h in 0.5 M H_2SO_4 with 0.25 g/L of MLA are shown in Fig. 6. Analysis of Fig.6 reveals less damage in the Cu surface in the presence of inhibitor and the image shows the formation of protective films by the adsorbed bioactive species on the metal surface.

3.3.2 EDXS analysis

The EDXS images of the uninhibited and inhibited copper specimens are shown in Fig.7 (a and b) and the analytical data are collected in Table 5. Both the specimens show the presence of Cu, O, Si, Zn, and S. Comparison of the data shows a higher percentage of copper in the inhibited copper specimen. This indicates adsorption of the inhibitor molecules on to the copper surface, preventing dissolution of metal ions in the aggressive medium.

3.4 Analysis of the FT-IR spectra

Fig. 8(a) shows the FT-IR spectrum of the dried MLA extract. The broad peak at 3355.66 cm^{-1} is due to the O-H and/or N-H stretching vibrations. The peaks at 1608 cm^{-1} and 1711 cm^{-1} could be assigned to C=O stretching and N–H bending vibrations respectively. The peak at 1452 cm^{-1} indicates the presence of coupled C–O stretching and O–H in-plane bending vibrations. The IR spectrum of the dried MLA has

been compared with the spectrum (Fig. 8 b) of the scrapped material from the copper surface after immersion in 0.5 M H_2SO_4 with MLA. A considerable positive or negative shift in the above-mentioned frequencies can be observed in the IR spectrum of the scrapped material. Hence, from the FT-IR and SEM-EDXS studies, it can be concluded that various organic constituents and groups with π electrons are effectively adsorbed on to the copper surface.

4 Conclusions

- Increasing the concentration of inhibitor increases the inhibition efficiency. The efficiency decreases with increasing temperature, which suggests the adsorption process follows physisorption.
- The inhibitor gives maximum efficiency at 72 h of immersion time.
- E_a values are found to be higher for the inhibited system than that for the uninhibited system, which also supports the physisorption of the inhibitor molecules on to the metal surface.
- The adsorption of the extract followed Langmuir isotherm.
- Polarization studies indicate that the inhibitor acts as a mixed type inhibitor.
- The adsorption of the inhibitor molecules on the MS surface is confirmed by the results of FT-IR and EDXS studies.
- The inhibition efficiency values obtained from weight loss measurements and electrochemical experiments are in good agreement.

Declarations

Ethics approval and consent to participate

Manuscripts reporting studies involving human participants and human data only.

Competing interests

We have no financial or personal interests to publish this paper,

Authors' contributions

Both the authors have equally contributed the written materials for preparing this manuscript.

Funding

No funding is received

Availability of data and materials

The datasets used and /or analyzed during the current study are available from the corresponding author on reasonable request.

References

1. Sherif. EM, Inhibition of copper corrosion reactions in neutral and acidic chloride solutions by 5-ethyl-1, 3, 4-thiadiazol-2-amine as a corrosion inhibitor, Corrosion. 2012,7,2832–2845.
2. Trabanelli.G, Inhibitors, An old remedy for a new challenge, Corrosion. 1991, 47(6), 410–419.
3. Anozie.I. U, Akoma. C. S, Nnanna. L. A, International Journal of Pure and Applied Sciences and Technology, (2011), 6(2), 79.
4. Khandelwal.R, Arora. S.K, Upadhayay. R. K, Mathur .S.P, Parashar .R, International Journal of Current Trends in Science and Technology, 3(2), (2012), 70.
5. Alaneme.K. K, Olusegun. S. J, Leonardo Journal of Sciences, 20 (2012), 59.
6. Olusegun. S.J, Adeiza.B. A, Ikeke. K. I, Bodunrin .M.O, Journal of Emerging Trends in Engineering and Applied Sciences, 4 (2013), 138.
7. Cang.H, Fei .Z, Shao. J, Shi. W, Xu. Q, International Journal of Electrochemical. Science, 8 (2013), 720.
8. Muthukrishnan.P, Jeyaprabha .B, Prakash .P, International Journal of Industrial Chemistry, (2014) 5:5DOI 10.1007/s40090-014-0005-9.
9. Eddy.N.O, Odiongenyi. A. O, Ameh.P. O, Ebenso .E. E, International Journal of Electrochemical. Science, 7 (2012), 7425.
10. Eduok. U.M, Umoren. S.A, Udoh. A.P, Arabian Journal of Chemistry, 5(2012), 325.
11. Latha. B, Rumaisa. Y, Soumya. C. K, Shafeena Shahul, and Sandhiya (2013) N, Journal of Chemical and Pharmaceutical Research, 5(4), 222–228.
12. Jyothi. S and Ravichandran. J (2015) Inhibitive action of the acid extract of *Luffa aegypticca* leaves on the corrosion of mild steel in acidic medium, Journal of Adhesion Science and Technology, 29(3), 207–231.
13. Khaled. KF (2003) The inhibition of benzimidazole derivatives on corrosion of iron in 1M HCl solutions. Electrochim Acta 48(17), 2493–2503.
14. McCafferty. E, Hackerman. N(1972) Double layer capacitance of iron and corrosion inhibition with polymethylene diamines. J Electrochemical Soc, 119(2), 146–154.
15. Krishnaveni. K, Ravichandran. J, Selvaraj. A (2013) Effect of Morindatinctoria leaves extract on the corrosion inhibition of mild steel in acid medium, Acta Metallurgica Sinica (English Letters) 26(3), 321–7.
16. Perumal. S, Muthumanickam. S, Elangovan. A Karthik. R, and Mothilal. K, *Bauhinia tomentosa* Leaves Extract as Green Corrosion Inhibitor for Mild Steel in 1 M HCl medium, Journal of Bio and Tribo-Corrosion, 2017, 3(2), 13.
17. Ali. A. L, ShMahrous. Y, Corrosion inhibition in acidic media from fruiting bodies of *Melia Azedarach* Leaves extract and synergistic Ni^{2+}additive. RSC Advances, 2017, 7(18), 23687–23698.

18. Aejitha. S, Kasthuri. P. K and Jyothi. S, corrosion inhibitory action of *Commiphora candata* extract on the mild steel corrosion in 1 M H_2SO_4 acid medium, Journal of adhesion science and Technology, 2016, 30, 784–802.
19. Abboud. Y, Tanane. O, ElBouari. A Salghi. R, Hammouti. B, Chetouani. A and Jodeh.S, Corrosion inhibition of carbon steel in a hydrochloric acid solution using pomegranate leave extract, Corrosion Engineering, Science and Technology, 2016, 51(8), 557–565.
20. Rahman. M. A, Islam. M. S (2013) Antioxidant, antibacterial and cytotoxic effects of the phytochemicals of whole *Leucas Aspera* extract, Asian Pacific journal of tropical biomedicine, 3(4), 273
21. Kavitha.N, Kathiravan. S, Jyothi. S, Murugesh. A, and Ravichandran .J, Adsorption and Inhibitive properties of Methanol extract of *Leucas Aspera* leave for the corrosion of Mild Steel in HCl medium, Journal of Bio and Tribo Corrosion, 2019,5(2), 51.
22. Leelavathi. S, Rajalakshmi. R, J. Mater. Environ. Sci, 4(5) (2013), *Dodonaea viscosa* (L.) Leaves extract as acid Corrosion inhibitor for mild Steel – A Green approach, 625–638.
23. Solomon. M, Umoren. M.S.A, Udosoro. I. I and Udoh. A. P (2010) Inhibitive and adsorption behaviour of carboxymethyl cellulose on mild steel corrosion in sulphuric acid solution, Corrosion Science, 52(4), 1317–1325
24. Oguzie. E.E(2005) Inhibition of acid corrosion of mild steel by *Telfaria occidentalis* extract. Pigment& Resin Technology, 34(6), 321–326
25. Obot.I.B, Obi-egbedi. N.O(2010) Adsorption properties and inhibition of mild steel corrosion in sulphuric acid solution by ketoconazole: experimental and theoretical investigation. Corros. Sci. 52(1), 198–204 (in English)
26. Manimegalai, S, and Manjula. P (2015) Thermodynamic and Adsorption studies for Corrosion Inhibition of Mild steel in Aqueous Media by Sargasamswartzii (Brown algae), Journal of Material and Environmental Science, 6(6), 1629–1637.
27. Shukla. S. K, Quraishi. M. A, Ebenso. E (E2011) Adsorption and corrosion inhibition properties of cefadroxil on mild steel in hydrochloric acid, International Journal of Electrochemical Science, 6, 2912-31.
28. Saker. S, Aliouane. N, Hammache. H, Chafaa. S and Bouet. G (2015) Tetraphosphoric acid on eco-friendly corrosion inhibitor on carbon steel in 3N NaCl aqueous solutions, Ionics, 21(7), 2079–2090.
29. Raja. PB, Sethuraman. MG (2008) Natural products as a corrosion inhibitor for metals in corrosive media – a review.Mater Lett, 62(1), 112–116.
30. Gunasekaran. G, Chauhan. L.R (2004) Eco-friendly inhibitor for corrosion inhibition of mild steel in phosphoric acid medium. Electrochimica Acta, 49(25), 4387–4395.

Tables

Table1. Effect of concentration of MLA on the corrosion of copper in 0.5 M H_2SO_4 from weight loss method

Conc. of MLA (g /L)	1 h		5 h		48 h		72 h	
	CR (mpy)	(%)IE	CR (mpy)	(%)IE	CR (mpy)	(%)IE	CR (mpy)	(%)IE
Blank	108.7		97.48		87.52		85.02	
0.05	71.22	34.48	61.54	36.86	53.22	39.19	47.52	44.1
0.10	63.72	41.37	50.28	48.42	44.21	49.48	41.72	50.92
0.15	48.73	59.97	38.11	60.9	33.74	61.44	29.39	65.43
0.20	41.23	62.06	36.21	62.85	31.33	64.2	26.88	68.38
0.25	33.73	68.96	29.96	69.26	21.01	75.89	19.22	77.39

Table .2. Effect of temperature on the corrosion of copper in 0.5 M H_2SO_4 with MLA

Conc. of MLA (g/L)	303 K		313 K		323 K		333 K	
	CR (mpy)	(%)IE	CR (mpy)	(%)IE	CR (mpy)	(%)IE	CR (mpy)	(%)IE
Blank	108.7		153.68		273.93		367.35	
0.05	71.22	34.48	104.95	31.71	198.66	27.47	307.37	16.32
0.10	63.72	41.37	101.2	34.14	187.42	31.58	296.12	19.39
0.15	48.73	59.97	86.21	43.9	176.17	35.68	284.88	22.44
0.20	41.23	62.06	78.71	48.78	149.93	45.26	281.13	23.47
0.25	33.73	68.96	74.96	51.22	146.19	46.63	269.89	26.53

Table 3. Values of activation energy and thermodynamic parameters for the corrosion of copper with and without different concentrations of MLA

S.No.	Conc.of MLA (g /L)	E_a (kJ mol^{-1})	$-\Delta G_{ads}$ (kJ mol^{-1})				$-\Delta H_{ads}$ (kJ mol^{-1})	ΔS_{ads} (kJ mol^{-1})
			303 K	313 K	323 K	333 K	-	-
1	Blank	35.50	-	-	-	-	32.49	0.0512
2	0.05	42.11	16.98	16.47	15.96	15.45	33.39	0.0582
3	0.10	43.81	15.76	15.18	14.60	14.01	49.78	0.1100
4	0.15	50.46	16.46	15.36	14.26	13.16	48.84	0.1079
5	0.20	53.70	16.16	15.08	14.00	12.92	52.70	0.1206
6	0.25	58.01	16.16	14.95	13.75	12.54	32.49	0.0512

Table.4. Electrochemical parameters for the corrosion of copper in 0.5 M H_2SO_4 at different concentrations of the inhibitor

Conc.of MLA (g /L)	PDP					EIS		
	b_a mV dec^{-1}	b_c mV dec^{-1}	$(-E_{corr})$ mV sec^{-1}	I_{corr} * 10^{-4} Amp cm^{-2}	% IE	R_{ct} Ωcm^2	C_{dl} * 10^{-5} Fcm^{-2}	IE
Blank	127.95	209.90	119.5	0.1599	-	565.5	4.868416	-
0.05	154.15	282.64	124.3	0.1450	9.31	586.5	5.590653	3.58
0.10	132.52	186.49	117.0	0.1425	10.88	736.5	3.371578	23.21
0.15	109.51	180.08	91.7	0.1364	14.69	920.9	2.62949	38.59
0.20	103.42	184.26	89.3	0.1187	25.76	1233	3.200132	54.13
0.25	98.96	176.14	81.3	0.1133	29.14	1388	2.332768	59.25

Table 5. EDXS analysis results of the copper specimen in 0.5 M H_2SO_4 in the absence and presence of MLA

H_2SO_4 medium	Composition (%)					
	Cu	O	Si	Zn	C	S
Cu in 0.5M H_2SO_4	64.13	15.48	3.13	5.92	9.76	1.58
Cu 0.5M H_2SO_4 +MLA	87.93	3.32	1.81	6.26	0.67	-

Figures

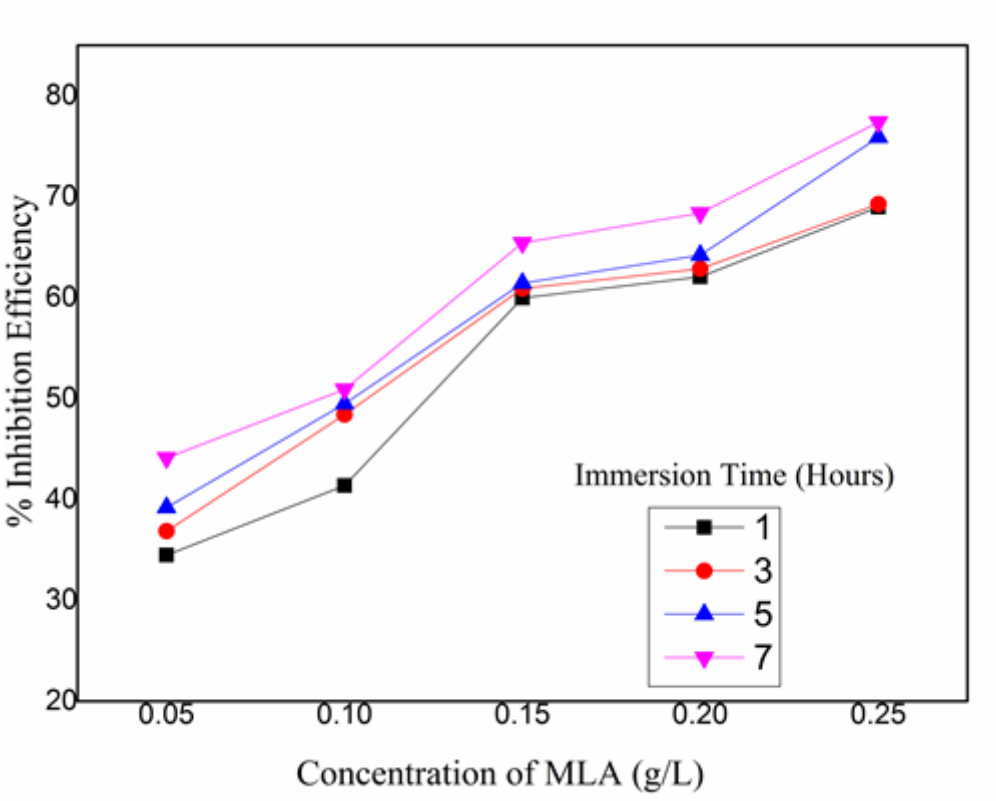

Figure 1

Effect of concentration of MLA on the corrosion of copper in 0.5 M H_2SO_4 from weight loss method

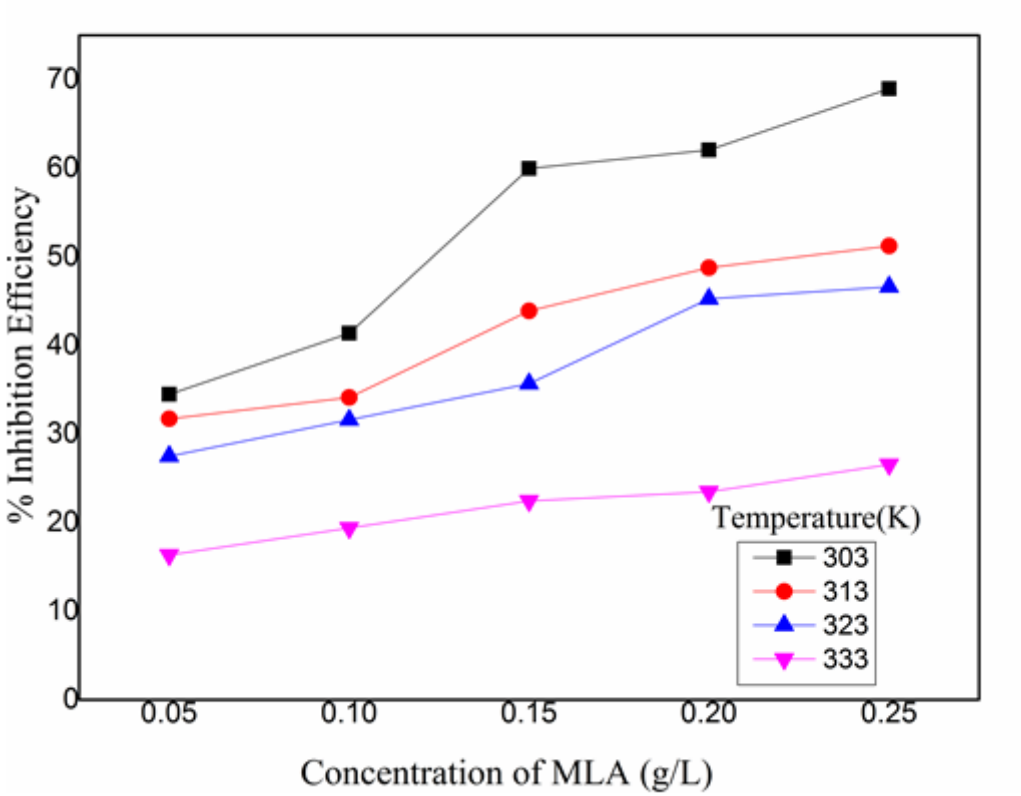

Figure 2

Effect of temperature on the corrosion of copper in 0.5 M H_2SO_4 with MLA

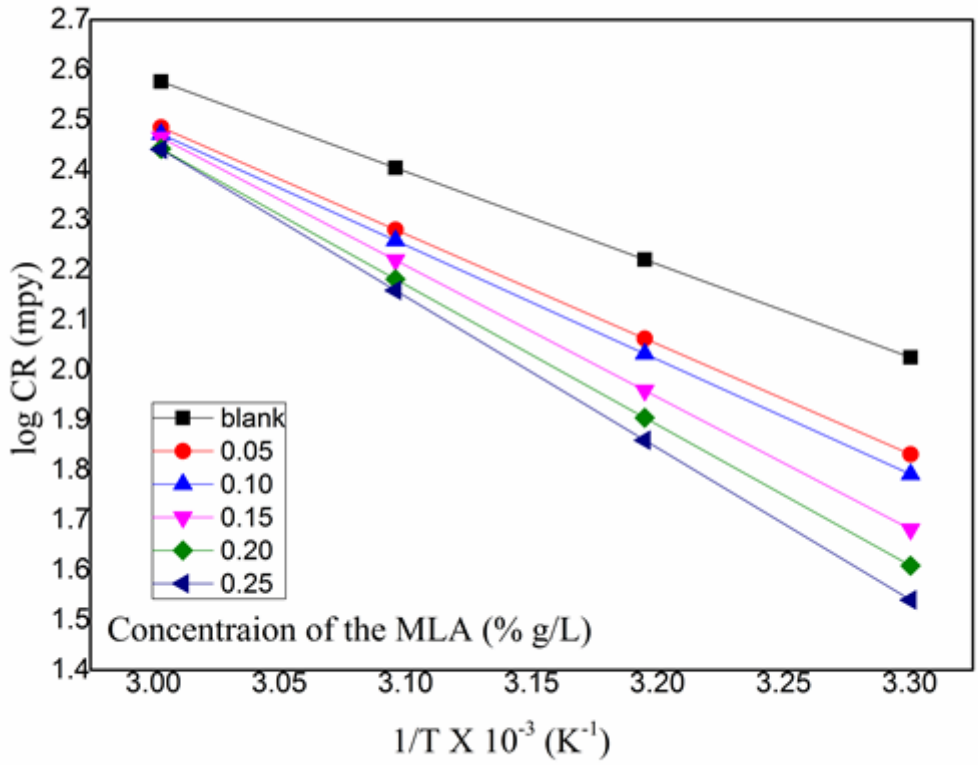

Figure 3

Arrhenius plots for the corrosion of copper in 0.5 M H_2SO_4 with MLA

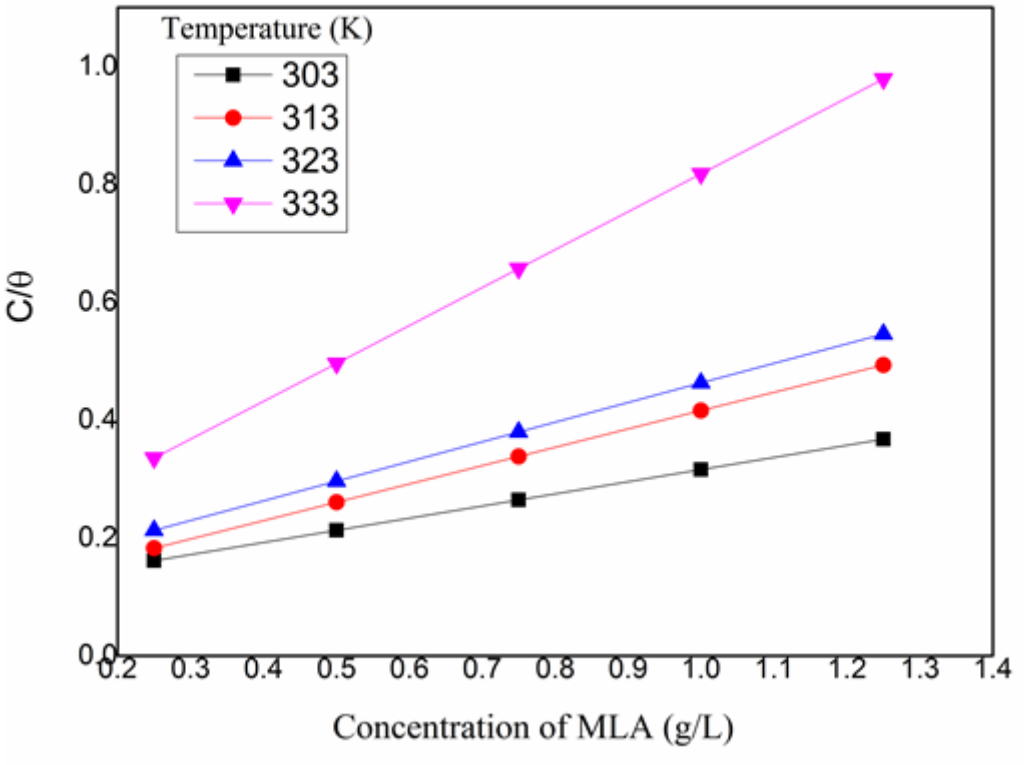

Figure 4

Langmuir adsorption isotherm for the corrosion of copper in 0.5 M H_2SO_4 with MLA

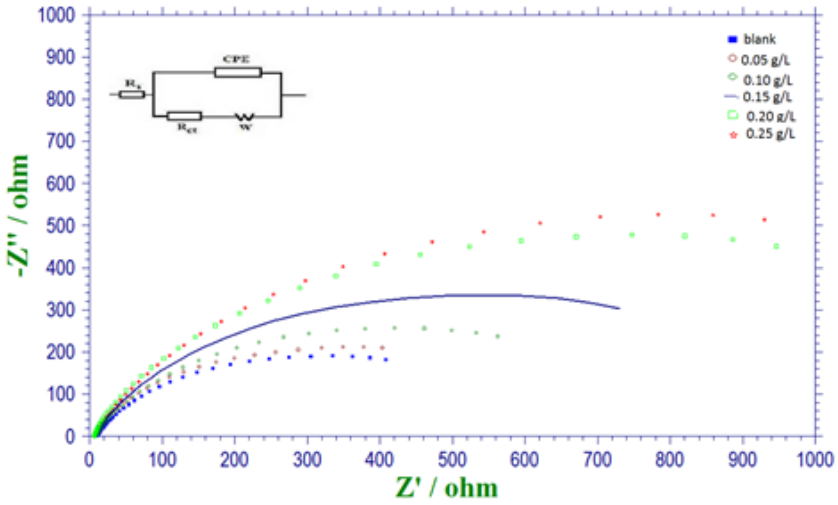

(a)

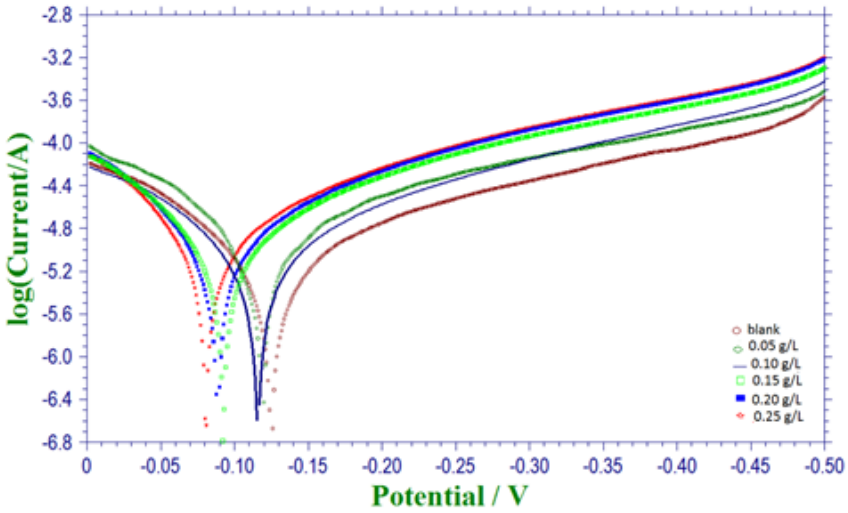

(b)

Figure 5

(a) Nyquist plots for the corrosion of copper in 0.5 M H_2SO_4 with various concentrations of MLA

(b) Tafel plots for the corrosion of copper in 0.5 M H_2SO_4 with various concentrations of MLA

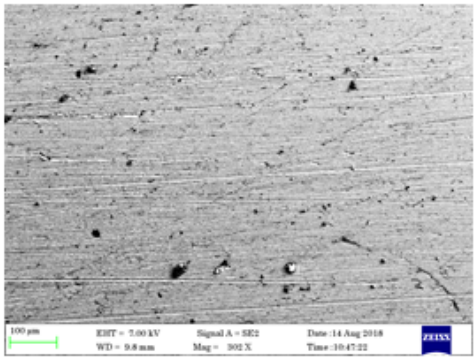

(a)

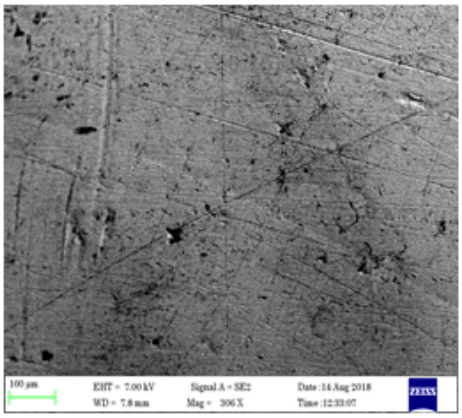

(b)

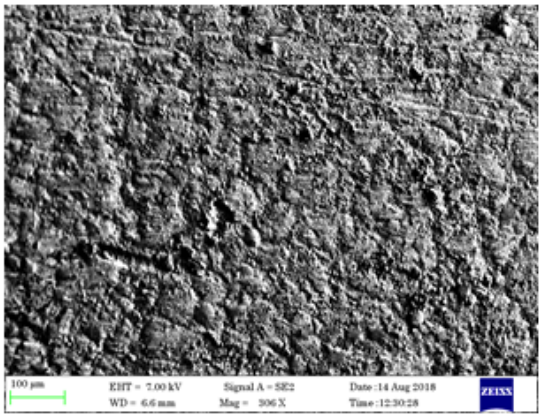

(c)

Figure 6

(a) SEM image of pure Cu sample

(**b**) SEM image of the copper sample exposed for 72 h in 0.5 M H_2SO_4

(c) SEM image of the copper sample exposed for 72 h in 0.5 M H_2SO_4 with MLA

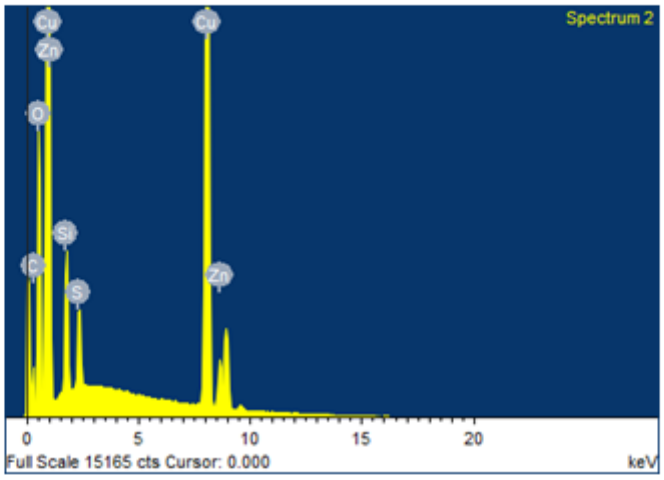

(a)

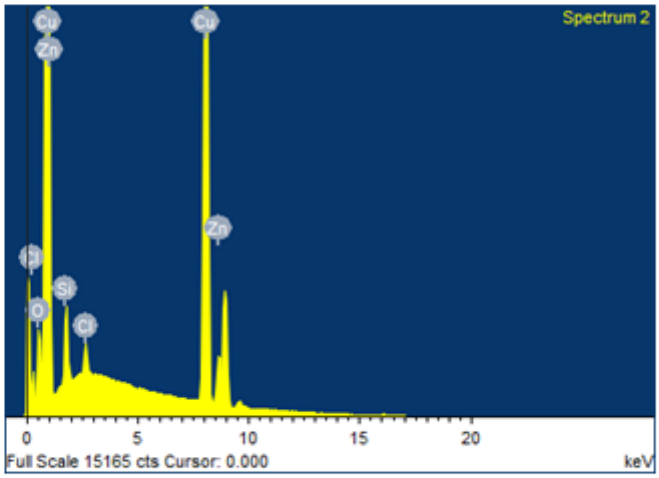

(b)

Figure 7

(a) The EDXS image of the copper sample exposed for 72 h in 0.5 M H_2SO_4

(b) The EDXS image of the copper sample exposed for 72 h in 0.5 M H_2SO_4 with MLA

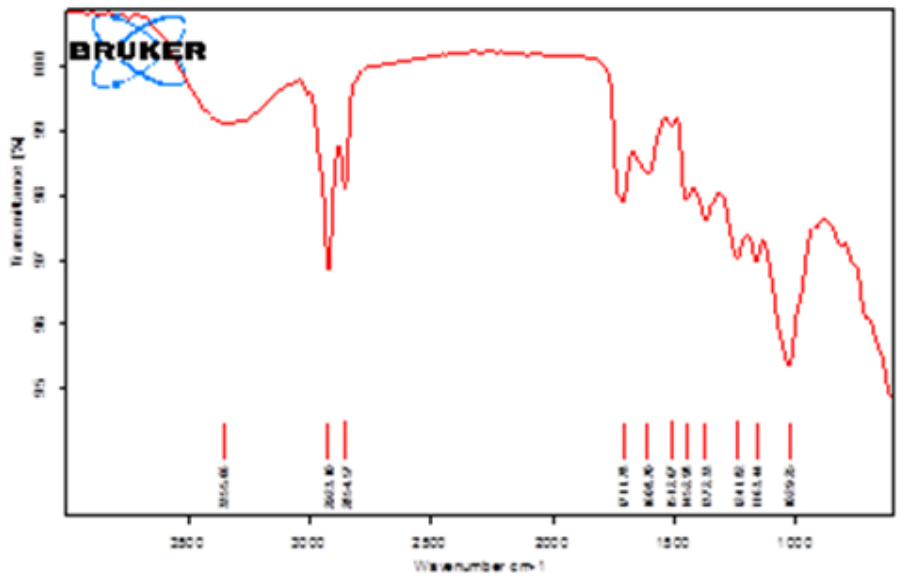

(a)

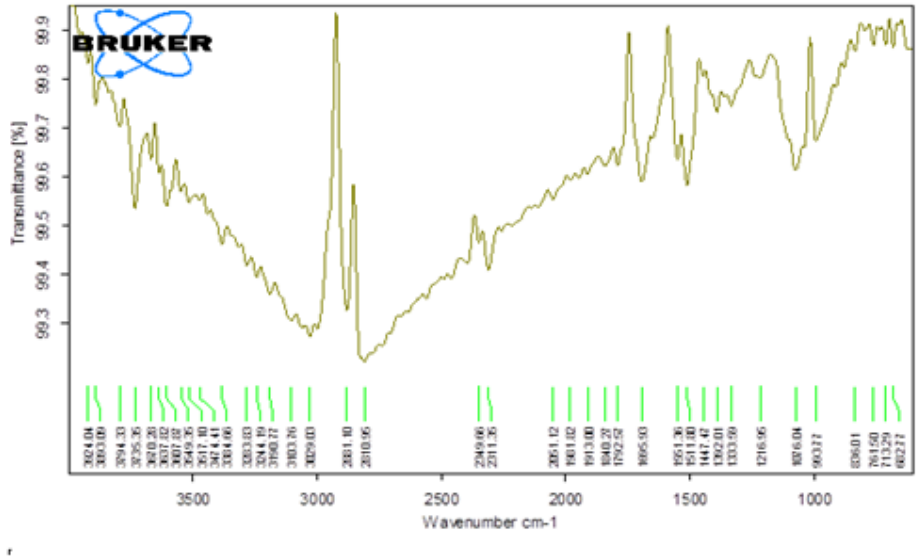

(b)

Figure 8

(a) FT-IR spectrum of the dried MLA extract

(b) FT-IR spectrum of the scrapped material from the copper surface after immersion in 0.5 M H_2SO_4 with MLA